

Low loss silicon fibers for photonics applications

Laura Lagonigro,¹ Noel Healy,¹ Justin R. Sparks,² Neil F. Baril,² Pier J. A. Sazio,¹ John V. Badding,² and Anna C. Peacock^{1,a)}

¹*Optoelectronics Research Centre, University of Southampton, Southampton SO17 1BJ, United Kingdom*

²*Department of Chemistry and Materials Research Institute, Pennsylvania State University, 16802 Pennsylvania, USA*

(Received 4 December 2009; accepted 21 December 2009; published online 27 January 2010)

Silicon fibers are fabricated using a high pressure chemical deposition technique to deposit the semiconductor material inside a silica capillary. The silicon is deposited in an amorphous state into pure silica capillaries and can be crystallized to polysilicon after the deposition via a high temperature anneal. Optical transmission measurements of various amorphous and polycrystalline core materials were performed in order to determine their linear losses. Incorporating silicon functionality inside the fiber geometry opens up new possibilities for the next generation of integrated silicon photonics devices. © 2010 American Institute of Physics.

[doi:[10.1063/1.3294630](https://doi.org/10.1063/1.3294630)]

Continuous advancements in silicon photonics have led to the demonstration of a number of compact optoelectronic devices. To date much of the progress in this area has been based on photolithographically defined single crystal silicon-on-insulator (SOI) devices. However, in an attempt to break the bottleneck of limited real estate, recently attention has turned to complementary metal-oxide-semiconductor (CMOS) compatible structures based on amorphous and polycrystalline silicon. Devices made of these materials are not only easier, but also much cheaper to fabricate making them ideal candidates for use in silicon interconnect technology. For example, using standard CMOS techniques researchers have demonstrated the fabrication of a vertically integrated polysilicon waveguide on a single chip.¹ As materials for photonics applications, most of the research on amorphous and polysilicon has focused on reducing the optical transmission losses.^{2,3} Nevertheless, some important active on-chip devices have been reported of late, including optical switches and modulators.^{4,5}

An alternative approach to the all optical planar integrated circuit is to incorporate the active semiconductor component into the fiber geometry so that signal processing functions can be carried out inside the data transport medium. Using a high pressure chemical processing technique bulk silicon has been deposited into the internal holes of pure silica capillaries to fabricate some of the earliest silicon optical fibers.⁶ Typically the silicon is deposited at low temperatures so that it forms in an amorphous state which can be crystallized to polysilicon after the deposition via a high temperature anneal. This simple and low cost fabrication procedure can be easily modified to fill a range of capillary sizes so that the waveguide dimensions can be optimized for the specific application.

In this letter we investigate the optical transmission losses of these silicon fibers with both amorphous and polysilicon core materials. Conditions are optimized to control the deposition of the semiconductor material which is important for obtaining both low loss amorphous and high quality polysilicon materials. For example, in conventional plasma

enhanced chemical vapor deposition (PECVD), the incorporation of hydrogen into the amorphous material is known to saturate the dangling bonds, thus reducing the absorption losses.⁷ Unfortunately, however, hydrogen is detrimental to the crystallization of polysilicon as it reduces the density of the silicon material so that it shrinks and detaches from the silica cladding as hydrogen is driven out during the high temperature anneal.⁸ Here we have compared a range of deposited materials and annealing conditions to establish key parameters to obtaining low loss silicon fibers. The results demonstrate the potential for both amorphous and polysilicon materials to be used in all-fiber networks.

The silicon fiber structures are fabricated by depositing the semiconductor material inside pure silica capillaries using a high pressure microfluidic chemical deposition technique.⁶ Glass capillaries make excellent templates for materials deposition as their mechanical strength allows them to withstand the extreme deposition conditions,⁹ they have especially smooth internal surfaces [0.1 nm root mean square roughness (Ref. 10)], and the hole dimensions can be easily scaled to the desired core size. The deposition process is conducted by forcing a mixture of silane and helium (SiH₄/He) to flow through the central hole under high pressures ~35 MPa and temperatures that range between 400–500 °C. At these temperatures the material deposits in an amorphous state which ensures that it bonds smoothly to the silica walls, thus minimizing the roughness at the silicon-silica interfaces.¹¹ If required, crystallization to polysilicon is then performed after the deposition process via annealing at temperatures up to 1325 °C.

The fibers used in our investigations are fabricated by depositing silicon inside capillaries with a ~6 μm inner diameter. Owing to the large index difference between the silicon core and silica cladding, the guided light is well confined to the micron sized core. Figure 1(a) shows a SEM micrograph of a silicon fiber where the core has been slightly etched out of the silica cladding to facilitate imaging. To obtain optimal coupling into and out of these fibers we first mount them inside thicker silica capillary tubes and then use a standard polishing technique to finish the end faces. Figure 1(b) shows an example of a polished fiber imaged using an

^{a)}Electronic mail: acp@orc.soton.ac.uk.

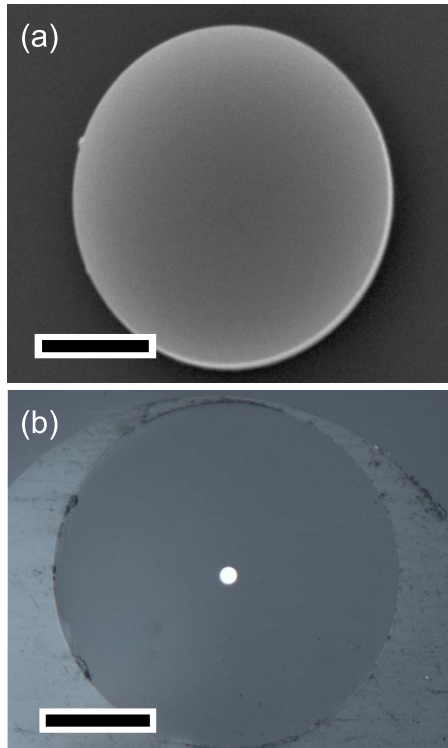


FIG. 1. (Color online) (a) SEM micrograph of a silicon fiber with the core slightly etched from the cladding; scale bar $2\ \mu\text{m}$. (b) Polished fiber for optical coupling, mounted inside a thicker capillary; scale bar $40\ \mu\text{m}$.

optical microscope. We consider five silicon fibers fabricated under different conditions: (A) amorphous silicon deposited at $\sim 400\ ^\circ\text{C}$, (B) amorphous silicon deposited at $\sim 500\ ^\circ\text{C}$, (C) polysilicon deposited at $\sim 500\ ^\circ\text{C}$ and annealed up to $1125\ ^\circ\text{C}$, (D) polysilicon deposited at $\sim 500\ ^\circ\text{C}$ and annealed up to $1200\ ^\circ\text{C}$, and (E) polysilicon deposited at $\sim 500\ ^\circ\text{C}$ and annealed up to $1325\ ^\circ\text{C}$.

To determine the quality of the deposited material of the various fibers we conducted micro-Raman measurements on the silicon rods. In all cases a $633\ \text{nm}$ HeNe laser was focused onto the silicon through the side of the transparent silica cladding, with a spot size of $\sim 2\ \mu\text{m}$ and $\sim 3\ \text{mW}$ of power at the outer surface, and the backscattered radiation recorded on a thermoelectrically cooled Horiba Jobin Yvon Synapse CCD detector. Figure 2(a) shows the Raman spectra of the two amorphous silicon fibers. Both fibers exhibit a strong broad peak around $480\ \text{cm}^{-1}$ corresponding to the transverse optical mode, with some weaker subsidiary peaks associated with the other known vibrational modes of amorphous silicon.¹² Interestingly, looking to the higher frequency regime, as shown in the inset, sample A (solid line) also has a peak at $\sim 2000\ \text{cm}^{-1}$ which is typically associated with the presence of hydrogen.¹³ This peak is absent in sample B (dashed line) indicating that, as in the case of PECVD, hydrogen may be incorporated into the amorphous material at low deposition temperatures.¹⁴ The effects of hydrogen incorporation via this method are currently under investigation and will be the subject of a future publication. However, based on this observation, we chose to only investigate polysilicon fibers that were annealed from amorphous samples deposited at $\sim 500\ ^\circ\text{C}$ to avoid the possibility of hydrogen out diffusion. The Raman spectra for the polysilicon samples are then shown in Fig. 2(b), together with a

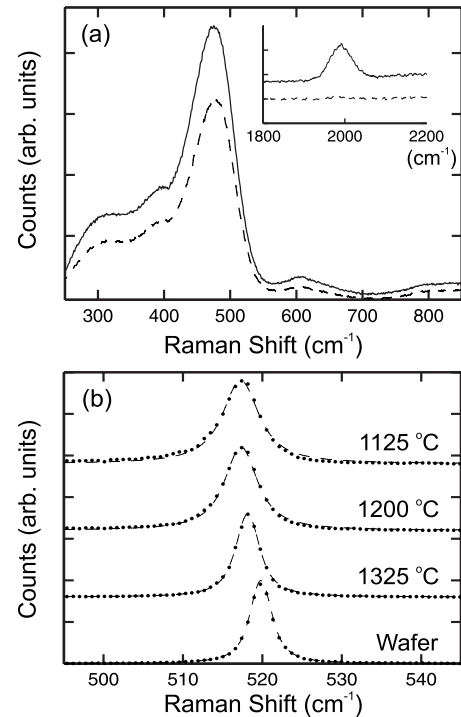


FIG. 2. (a) Raman spectra for the amorphous silicon fibers; sample A (solid curve) and sample B (dashed curve). Inset indicates the presence of hydrogen in sample A. (b) Raman spectra of the polysilicon fibers (top 3 curves) and a single crystal silicon wafer (bottom curve). Dashed lines are Voigt fits.

reference spectrum taken of a single crystal silicon wafer (bottom curve). To estimate the Raman peak widths, the spectra are fitted with Voigt profiles (dashed curves) to account for the $1.5\ \text{cm}^{-1}$ Gaussian instrument contribution. The silicon wafer has a Lorentzian FWHM of $2.7\ \text{cm}^{-1}$, centered at $520\ \text{cm}^{-1}$, with the polysilicon widths measured to be $5.1\ \text{cm}^{-1}$, $4.5\ \text{cm}^{-1}$, and $3.0\ \text{cm}^{-1}$ for samples C ($1125\ ^\circ\text{C}$ anneal), D ($1200\ ^\circ\text{C}$ anneal), and E ($1325\ ^\circ\text{C}$ anneal), respectively. The larger widths and the asymmetries seen in the polysilicon peaks, particularly for the lower temperature annealed samples, are due to contributions from the defect and amorphous materials, that surround the single crystal grains, which are associated with vibrations at frequencies in the range $500\text{--}517\ \text{cm}^{-1}$.¹⁵ We attribute the smaller width of the Raman peak of sample E to a reduction in the defect and amorphous content, and hence an improvement in the overall crystallinity.² From previous depositions with similar linewidths we anticipate the crystal grain sizes to be of the order $0.5\text{--}1\ \mu\text{m}$.^{6,16} While the slight red shift of the polysilicon peaks ($517\ \text{cm}^{-1}$ for samples C and D, and $518\ \text{cm}^{-1}$ for sample E) is, in part, due to the material surrounding the crystal grains, we also expect there to be a small contribution from the residual stress induced across the silicon-silica boundaries which are introduced during annealing, and are a result of the differences in the thermal expansion of the strongly bonded materials.¹⁶

Optical transmission losses of the fibers as a function of the guided wavelength were determined using a cut-back method, where the typical starting length was $\sim 8\ \text{mm}$ and we polished $1\ \text{mm}$ off the samples between each measurement. A supercontinuum source was filtered using a tunable acousto-optic device to yield an average power of $\sim 0.5\ \text{mW}$ over the wavelength range $1.2\text{--}1.7\ \mu\text{m}$, and launched into the silicon cores via free space coupling using a $25\times$ micro-

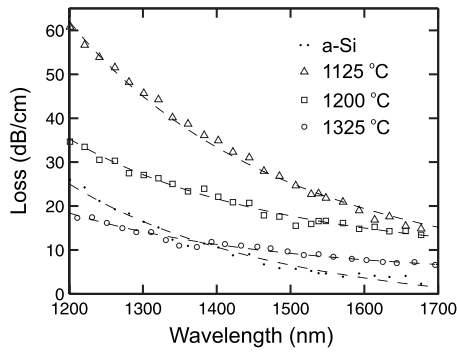


FIG. 3. Transmission losses as a function of wavelength for amorphous sample (A) and polysilicon samples (C) 1125 °C, (D) 1200 °C, and (E) 1325 °C. Dashed lines are λ^{-4} fits.

scope objective lens. A second 40 \times objective is used to capture the transmitted light and focus it onto a Newport 2832C power meter. The results of the loss measurements are plotted in Fig. 3 for all but the amorphous sample B. Without hydrogen to saturate the dangling bonds, amorphous silicon is highly lossy over the infrared wavelength range and the large loss of 50 dB/cm at 1550 nm measured in sample B is not unexpected. At wavelengths less than 1550 nm the losses in this fiber increase dramatically so that most or all of the transmitted light is absorbed, while at the longer wavelengths the measurements were limited by the detector sensitivity.

From the curves measured for the remaining samples, it is clear that in all cases the losses decrease for increasing wavelength, which suggests that scattering mechanisms contribute significantly. Further evidence to this is provided by the good agreement with the fitted curves which display the λ^{-4} dependence associated with Rayleigh scattering, which is in accordance with previous measurements.^{2,17} Comparison of the polysilicon loss curves shows that there is a clear reduction in the losses as the annealing temperature is increased, which follows from our earlier Raman observations that the higher temperature anneal leads to an improvement in the polycrystalline quality. From sample E, we determine the loss at 1550 nm to be ~ 8 dB/cm, which is close to the lowest loss measured in a polysilicon fiber.⁶ Although the amorphous sample A shows a similar wavelength dependence, the slope of this data set is much steeper than the two higher temperature annealed samples which we expect to be predominantly crystalline in nature. Thus we attribute the sharp increase in the losses at short wavelengths in the low temperature anneal sample C to a contribution from the amorphous silicon material which surrounds the crystal grains. Significantly, sample A yields the lowest loss of ~ 5 dB/cm at 1550 nm, which suggests that the incorporation of hydrogen, which was evident from the Raman curve, has resulted in an appreciable saturation of dangling bonds in the material.

The results of the transmission measurements indicate that by further optimizing the deposition and annealing processes to obtain either high quality low loss amorphous silicon or polysilicon core materials, it should be possible to obtain silicon fibers with losses that approach those of the lowest recorded values in on-chip waveguides of around a few decibels per centimeter.^{7,18} The observed reduction in optical losses as the transmission wavelength increases suggests that silicon device performance and efficiency can be improved by operating at longer wavelengths. The versatile nature of the deposition technique to deposit a range of silicon materials inside the capillary template opens up new possibilities for the next generation of integrated silicon photonics devices for all-fiber networking.

The authors acknowledge EPSRC (Grant No. EP/G028273/1), NSF (Grant No. DMR-0806860), and the Penn State Materials Research Science and Engineering Center (NSF Grant No. DMR-0820404) for financial support. A.C.P. is a holder of a Royal Academy of Engineering fellowship.

- ¹K. Preston, B. Schmidt, and M. Lipson, *Opt. Express* **15**, 17283 (2007).
- ²L. Liao, D. R. Lim, A. M. Agarwal, X. M. Duan, K. K. Lee, and L. C. Kimerling, *J. Electron. Mater.* **29**, 1380 (2000).
- ³A. Harke, M. Krause, and J. Mueller, *Electron. Lett.* **41**, 1377 (2005).
- ⁴K. Preston, P. Dong, B. Schmidt, and M. Lipson, *Appl. Phys. Lett.* **92**, 151104 (2008).
- ⁵F. G. Della Corte, S. Rao, M. A. Nigro, F. Suriano, and C. Summonte, *Opt. Express* **16**, 7540 (2008).
- ⁶P. J. A. Sazio, A. Amezcua-Correa, C. E. Finlayson, J. R. Hayes, T. J. Scheidemantel, N. F. Baril, B. R. Jackson, D.-J. Won, F. Zhang, E. R. Margine, V. Gopalan, V. H. Crespi, and J. V. Badding, *Science* **311**, 1583 (2006).
- ⁷G. Cocorullo, F. G. Della Corte, R. De Rosa, I. Rendina, A. Rubino, and E. Terzini, *IEEE J. Sel. Top. Quantum Electron.* **4**, 997 (1998).
- ⁸Z. Remeš, M. Vaněček, A. H. Mahan, and R. S. Crandall, *Phys. Rev. B* **56**, R12710 (1997).
- ⁹C. R. Kurkjian, J. T. Krause, and M. J. Matthewson, *J. Lightwave Technol.* **7**, 1360 (1989).
- ¹⁰P. J. Roberts, F. Couny, H. Sabert, B. J. Mangan, D. P. Williams, L. Farr, M. W. Mason, A. Tomlinson, T. A. Birks, J. C. Knight, and P. St. J. Russell, *Opt. Express* **13**, 236 (2005).
- ¹¹L. Lagonigro, N. V. Healy, J. R. Sparks, N. F. Baril, P. J. A. Sazio, J. V. Badding, and A. C. Peacock, *CLEO/Europe-EQEC CE3* (2009).
- ¹²D.-J. Won, M. O. Ramirez, H. Kang, V. Gopalan, N. F. Baril, J. Calkins, J. V. Badding, and P. J. A. Sazio, *Appl. Phys. Lett.* **91**, 161112 (2007).
- ¹³M. H. Brodsky, M. Cardon, and J. J. Cuomo, *Phys. Rev. B* **16**, 3556 (1977).
- ¹⁴R. Sun, K. McComber, J. Cheng, D. K. Sparacin, M. Beals, J. Michel, and L. C. Kimerling, *Appl. Phys. Lett.* **94**, 141108 (2009).
- ¹⁵A. A. Parr, D. J. Gardiner, R. T. Carline, D. O. King, and G. M. Williams, *J. Mater. Sci.* **36**, 207 (2001).
- ¹⁶C. E. Finlayson, A. Amezcua-Correa, P. J. A. Sazio, N. F. Baril, and J. V. Badding, *Appl. Phys. Lett.* **90**, 132110 (2007).
- ¹⁷N. Healy, J. R. Sparks, M. N. Petrovich, P. J. A. Sazio, J. V. Badding, and A. C. Peacock, *Opt. Express* **17**, 18076 (2009).
- ¹⁸Q. Fang, J. F. Song, S. H. Tao, M. B. Yu, G. Q. Lo, and D. L. Kwong, *Opt. Express* **16**, 6425 (2008).